



**HAL**  
open science

## Small microplastics as a main contributor to plastic mass balance in the North Atlantic subtropical gyre

Marie Poulain, Matthieu Mercier, Laurent Brach, Marion Martignac, Corinne Routaboul, Emile Perez, Marie Christine Desjean, Alexandra ter Halle

### ► To cite this version:

Marie Poulain, Matthieu Mercier, Laurent Brach, Marion Martignac, Corinne Routaboul, et al.. Small microplastics as a main contributor to plastic mass balance in the North Atlantic subtropical gyre. *Environmental Science and Technology*, 2019, 53 (3), pp.1157-1164. 10.1021/acs.est.8b05458. hal-02399962

**HAL Id: hal-02399962**

**<https://hal.science/hal-02399962>**

Submitted on 10 Dec 2019

**HAL** is a multi-disciplinary open access archive for the deposit and dissemination of scientific research documents, whether they are published or not. The documents may come from teaching and research institutions in France or abroad, or from public or private research centers.

L'archive ouverte pluridisciplinaire **HAL**, est destinée au dépôt et à la diffusion de documents scientifiques de niveau recherche, publiés ou non, émanant des établissements d'enseignement et de recherche français ou étrangers, des laboratoires publics ou privés.



## Open Archive Toulouse Archive Ouverte

OATAO is an open access repository that collects the work of Toulouse researchers and makes it freely available over the web where possible

This is an author's version published in: <http://oatao.univ-toulouse.fr/23307>

**Official URL:**

<https://doi.org/10.1021/acs.est.8b05458>

**To cite this version:**

Poulain, Marie and Mercier, Matthieu and Brach, Laurent and Martignac, Marion and Routaboul, Corinne and Perez, Emile and Desjean, Marie Christine and Ter Halle, Alexandra Small microplastics as a main contributor to plastic mass balance in the North Atlantic subtropical gyre. (2019) Environmental Science & Technology, 53 (3). 1157-1164. ISSN 0013-936X

Any correspondence concerning this service should be sent to the repository administrator: [tech-oatao@listes-diff.inp-toulouse.fr](mailto:tech-oatao@listes-diff.inp-toulouse.fr)

# Small Microplastics As a Main Contributor to Plastic Mass Balance in the North Atlantic Subtropical Gyre

Marie Poulain,<sup>†,‡</sup> Matthieu J. Mercier,<sup>†</sup> Laurent Brach,<sup>‡</sup> Marion Martignac,<sup>‡</sup> Corinne Routaboul,<sup>§</sup> Emile Perez,<sup>‡</sup> Marie Christine Desjean,<sup>||</sup> and Alexandra ter Halle<sup>\*,‡</sup>

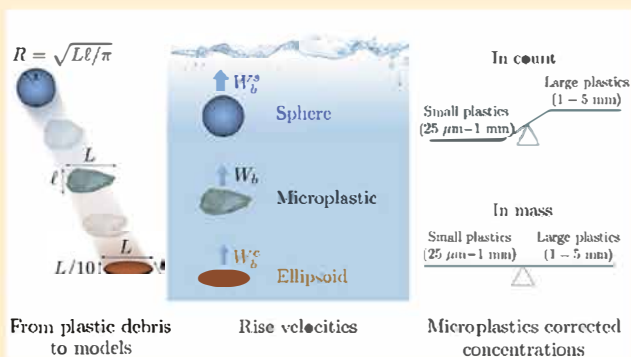
<sup>†</sup>Institut de Mécanique des Fluides de Toulouse (IMFT), Université de Toulouse, CNRS, Toulouse, France

<sup>‡</sup>Laboratoire des IMRCP, Université de Toulouse, CNRS UMR 5623, Université Paul Sabatier, 118 route de Narbonne 31062 Toulouse Cedex 9 France

<sup>§</sup>Institut de Chimie de Toulouse (ICT), Université de Toulouse, Université Paul Sabatier, 118 route de Narbonne 31062 Toulouse Cedex 9 France

<sup>||</sup>Centre National d'Études Spatiales, 18 avenue Édouard Belin, 31401 Toulouse cedex 4 France

**ABSTRACT:** Estimates of cumulative plastic inputs into the oceans are expressed in hundred million tons, whereas the total mass of microplastics afloat at sea is 3 orders of magnitude below this. This large gap is evidence of our ignorance about the fate of plastics, as well as transformations and sinks in the oceans. One of the current challenges consists of identifying and quantifying plastic particles at the microscale, the small microplastics (SMP, 25–1000  $\mu\text{m}$ ). The aim of the present study is to investigate SMP concentration in count and in mass at the sea surface in the North Atlantic subtropical gyre during the sea campaign Expedition 7<sup>th</sup> Continent. After isolation, SMP were characterized by micro Fourier transform infrared spectroscopy. Microplastic distribution was modeled by a wind driven vertical mixing correction model taking into account individual particle properties (dimension, shape and density). We demonstrate that SMP buoyancy is significantly decreased compared to the large microplastics (LMP, 1–5 mm) and consequently more susceptible to vertical transport. The uncorrected LMP concentration in count was between 13 000 and 174 000 pieces  $\text{km}^{-2}$ , and was between 5 and 170 times more abundant for SMP. With a wind driven vertical mixing correction, we estimated that SMP were 300 to 70 000 times more abundant than LMP. When discussing this in terms of weight after correction, LMP concentrations were between 50 and 1000  $\text{g km}^{-2}$ , and SMP concentrations were between 5 and 14 000  $\text{g km}^{-2}$ .



## ■ INTRODUCTION

Plastic production has had an amazing exponential growth since its industrialization in the 1950s. However, only 40 years later, we realized that we do not control plastic's end of life and have not put forth sufficient effort to promote its recycling. In the 2010s, the annual plastic input into the ocean was estimated to be 10 million tons.<sup>1</sup> None of the commonly used plastics are biodegradable, and thus, they tend to accumulate once discarded in the environment.<sup>2</sup> With solar illumination and mechanical forcing, plastic waste is oxidized and fragmented into smaller and smaller particles, reaching the nanoscale.<sup>3</sup> Currently, one important scientific question is how to balance the annual input into the oceans, which is one hundred of times more than the amount we are actually able to locate. This large gap is evidence of our critical lack of knowledge about the fate of plastic in the ocean. Efforts to detect plastic particles at the micro and nanoscales are needed.<sup>4,5</sup> Published works state that small microplastics

(SMP, 25–1000  $\mu\text{m}$ ) are present in the natural environment<sup>6,7</sup> and that they are genuinely more abundant than large microplastics (LMP, 1–5 mm).<sup>8,9</sup> However, until now, there has been no estimation of the weight SMP could represent at sea.

The scientific community has agreed that the characterization of SMP by visual detection and manual sorting is prone to significant errors.<sup>6,10–12</sup> For the detection and quantification of SMP, micro Fourier transform infrared ( $\mu$  FTIR) and micro Raman spectroscopy are promising tools that should be considered. The development of  $\mu$  FTIR and its suitability were demonstrated with spiked natural samples.<sup>13</sup> This technique was also applied successfully to address SMP

concentration in count in environmental samples. However, the data are still scarce, and studies have been conducted with marine sediments,<sup>14</sup> lagoon sediment,<sup>15</sup> coastal waters<sup>6</sup> and wastewater treatment plant<sup>16</sup> samples. From these studies, it is apparent that SMP outnumber LMP, but the SMP weight concentration basis was not discussed. SMP weight estimates have only been discussed on the basis of emission scenarios.<sup>17</sup>

Another specific issue discussed here is how to properly estimate the abundance of plastic particles at sea in the water column at a given location by the extrapolation of sea surface samples. The sea surface state, with turbulence induced by wind and waves or some specific flows,<sup>18</sup> can mix the upper water column and transport plastic particles vertically. This effect has been rationalized by turbulent models based on the assumption of a balance between the upward flux of particles due to buoyancy and the downward flux due to turbulence.<sup>19–21</sup> These models rely on the rise velocity of plastic,  $W_b$ , and turbulence modeling. The simplest approach consists of using a mean rise velocity of  $0.01 \text{ m s}^{-1}$  for all plastic particles.<sup>19</sup> However, laboratory measurements of  $W_b$  for plastic debris between 0.5 and 207 mm are evidence of important variations with ratios up to a factor 40; smaller particles rising slower.<sup>22</sup> Enders et al used a sphere to model microplastic (25  $\mu\text{m}$  to 5 mm) buoyancy and demonstrated that LMP can be mixed over a few meters, whereas SMP could be transported down to hundreds of meters at the same sea state.<sup>21</sup> Improvements to current modeling approaches are still highly necessary to better quantify concentration and mass estimates in open oceans.<sup>4,23</sup> The present study investigates SMP and LMP composition, count and weight concentrations in the North Atlantic subtropical gyre at the sea surface. SMP were characterized and numbered by  $\mu$  FTIR. A wind driven vertical mixing correction was developed to account for individual particle properties (density and geometry). Owing to the very dispersed geometry and density of microplastics, our modeling approach provided lower and upper bounds for the concentrations. The results with and without wind driven mixing were discussed.

## ■ MATERIALS AND METHODS

**Chemicals.** High density polyethylene (PE) pellets (CAS# 9002–88–4), poly(ethylene terephthalate) (PET) pellets (CAS# 25038–59–9, density of  $1.68 \text{ g mL}^{-1}$ ), poly(vinyl chloride) (PVC) powder (CAS# 9002–86–2, density of  $1.4 \text{ g mL}^{-1}$  at  $25 \text{ }^\circ\text{C}$ ), poly(methyl methacrylate) (PMMA) (CAS# 90011–14–7, an average molecular weight of 120 000), Nylon 6/6 pellets (CAS# 25038–54–4, density of  $1.14 \text{ g mL}^{-1}$  at  $25 \text{ }^\circ\text{C}$ ) and Nylon 12 (CAS# 25038–74–8, density of  $1.14 \text{ g mL}^{-1}$  at  $25 \text{ }^\circ\text{C}$ ) were purchased from Sigma Aldrich (Saint Louis, MO). Polystyrene (PS) pellets (3.5 mm) (CAS# 9003–53–6 PS), polypropylene (PP) pellets (3 mm) (CAS# 9003–07–0, melting flow index of 0.4 g per 10 min), low density PE pellets (1 mm), nonexpanded polyurethane (PU), and foam were purchased from Goodfellow (Huntingdon, UK). Sodium dodecyl sulfate (ACS reagent, >99%) and sodium hydroxide pellets were purchased from Sigma Aldrich (Saint Louis, MO).

**Microplastic Sampling and Extraction.** Plastic particles were collected from the sailing vessel Guyavoile in the North Atlantic subtropical gyre in June 2015 during the French sea campaign Expedition 7<sup>th</sup> Continent.<sup>24</sup> LMP were collected using a Neuston net with a rectangular frame ( $0.5 \times 0.4 \text{ m}$ ) fitted with a 2 m long net with a standard mesh size of 300  $\mu\text{m}$ .

LMP were collected from the surface layer at a depth of [0–20] cm. Tow durations were set to 30 min, and tows were all undertaken while the vessel was traveling at a speed of 1–2.5 knots. On the boat, the content of the tows was filtered on 300  $\mu\text{m}$  sieves. Most of the plastic particles were removed with tweezers and stored at  $-5 \text{ }^\circ\text{C}$  in glass vials. In total, 40 nets were towed: 12 outside the accumulation area and 28 within the accumulation area. The GPS locations and sea states associated with these 28 stations are supplied in the [Supporting Information \(SI\), Table S1](#). SMP were collected using a Neuston net with a standard mesh size of 25  $\mu\text{m}$ . The net was fixed to a  $0.3 \times 0.1 \text{ m}$  rectangular frame and was 3 m long. SMP were collected from the surface layer at a depth of [0–6] cm. Tow durations were set to 10 min and were all undertaken while the vessel was traveling at a speed of less than 1 knot. Indeed, the speed of the boat was strictly restricted to below 1 knot to avoid clogging the 25  $\mu\text{m}$  net. The net was towed from a zodiac boat, and for security reasons, it was only possible when the sea was relatively calm. Thus, only eight measurements were performed within the accumulation area. The content of the tows was filtered through a cellulose acetate membrane (5  $\mu\text{m}$ ) in a closed filtration unit and immediately stored in closed glass vials at  $-18 \text{ }^\circ\text{C}$ . Both manta nets were equipped with flow meters from which sea concentrations in count were calculated and expressed as numbers of particles per square kilometer.

**Microplastic Isolation.** The sorting and numbering of LMP were carried out classically and described elsewhere.<sup>24</sup> To calculate LMP sea surface concentrations (in count and weight), only those having at least one dimension above 1 mm were considered. For SMP isolation, the acetate filters obtained on the boat were immersed under laboratory conditions in 80 mL ultrapure water in a closed glass bottle at ambient temperature under gentle agitation for 1 h. After removal of the filter, the biogenic matter was eliminated by the addition of 20 mL of a  $10 \text{ mol L}^{-1}$  NaOH solution and 300  $\mu\text{L}$  of a  $50 \text{ g L}^{-1}$  sodium dodecyl sulfate solution. The solution was gently agitated for 4 h and stored for 1 week at ambient temperature. After 1 week, the solution was filtered through glass filters in a closed unit (Whatman GF/F; 0.7  $\mu\text{m}$ ; 47 mm) and rinsed abundantly with ultrapure water. The filters were then stored in closed glass Petri dishes prior to analysis. A control experiment under these conditions was performed to ensure that the plastic was not altered. (PET, PVC, PS, PE, PP, PU expanded or foam, Nylon6, Nylon12, and PMMA) were grinded at 200  $\mu\text{m}$  using a ZM 200 grinder (Retsch, Haen, Germany). The plastic powder (300 mg) was treated with sodium hydroxide under the same conditions.

**SMP Characterization by  $\mu$ -FTIR.** Micro FTIR spectroscopy was performed using a Thermo Fisher Scientific Nicolet iN10 apparatus in reflection mode equipped with a liquid nitrogen cooled MCT detector. The particle bigger than 30  $\times$  30  $\mu\text{m}$  visually detected by the operator under the microscope were analyzed. We cannot estimate how many particles could be missed by the operator, this is the most problem of working with an operator. All the work done those past two years by Primpke et al. are a huge improvement of the method. In the future we will work like this team. The spectra were recorded as the average of 16 scans in the spectral range of 650–4000  $\text{cm}^{-1}$  at a resolution of 8  $\text{cm}^{-1}$ . The library was from the Thermo Scientific software (database: Hummel Polymer library, HR Polymer and additives, HR Polymer additives and plasticizers). Each particle was identified and analyzed

individually. The microscope aperture was adapted to each particle. If the particle was suspected to be plastic, several measurements at different spots were undertaken to prevent false signals due to either local impurities or the rough and irregular shapes of the particles, which could alter their spectra. The plastic particles were identified using a polymer spectral library if the match was greater than 80% (by the software OMNIC PICTA with no normalization or derivation).

**Microplastic Geometrical Description.** We have identified two families of objects: lines and pieces. Lines were less numerous than pieces (14.6% for the LMP and 6.6% for the SMP). Here, we only consider pieces, and lines were excluded from the calculation.

We measured the length ( $L$ ), width ( $I$ ) and mass ( $M$ ) to the nearest 0.01 mg using a precise scale (Genius shatorius, Göttingen, Germany). In addition, for 415 microplastics (the sum of LMP and SMP) collected during a previous sea campaign in the North Atlantic subtropical gyre,<sup>26</sup> we also measured the thickness ( $h$ ) and the apparent surface area ( $S_a$ ) using image analysis (ImageJ<sup>®</sup>). A complete description is given in [SI Section S2](#).

**Rise Velocity Measurements.** Rise velocity measurements of LMP samples collected were done in the laboratory. A cylindrical tank (diameter, 13 cm and height, 100 cm) was filled with 18 L of fresh ( $1.001 \text{ g cm}^{-3}$ ) or salt water ( $1.025 \text{ g cm}^{-3}$ ). A single particle was inserted at the bottom of the column using a double valve system. The particle raised in the quiescent fluid (no residual flow observed). Passing times of the particle at three marks (50, 70, and 80 cm away from the bottom) were recorded in order to calculate  $W_b$ . We verified that the particle had reached a steady velocity, and each measurement was repeated four times, leading to less than 5% of uncertainty on  $W_b$ .

## ■ RESULTS AND DISCUSSION

**Microplastic Characterization.** LMP and SMP have been sampled at the sea surface of the North Atlantic subtropical gyre during the cruise Expedition 7<sup>th</sup> Continent. LMP extraction and numbering are classical procedures and have been described previously.<sup>27</sup> For SMP characterization, an essential first step of purification is needed to eliminate organic matter (algae, plankton) and inorganic particles (sand and silt) before detection. Very diverse purification approaches have been developed; all methods consist of several steps using density separation together with degradation of the organic matter.<sup>11,28,29</sup> Organic matter is eliminated by strong acidic<sup>21,30</sup> or alkaline<sup>31</sup> solutions, by oxidation agents<sup>13</sup> or by the use of enzymes.<sup>32</sup> We underline that the purification step needs to be as efficient as possible to facilitate spectroscopic detection without damaging the plastic particles by breaking them down or by altering the structure of the polymer, that is, conditions should remain mild. For SMP isolation, a sodium hydroxide treatment was chosen. As a control, 10 different polymers were ground ( $500 \mu\text{m}$ ) and tested with the sodium hydroxide treatment. Recoveries were higher than 95% ( $\pm 5\%$ ). Under the microscope, the treated polymer did not appear to be altered (no yellowing), and the  $\mu$  FTIR spectra of the treated plastics were not modified. Procedural blank experiments have been conducted: no plastic particles or cloth fibers have been detected in these control experiments. After purification and filtration, the particles deposited on the filter are analyzed by microspectroscopy. Both FTIR and Raman provide vibrational fingerprint spectra with information about the shape and

dimension of the particles. The techniques present a spatial resolution in the micrometric range and both methods have advantages and disadvantages for the detection of SMP. Their use in combination has been proposed by Kaeppler et al.<sup>33</sup> The detection and characterization of SMP by  $\mu$  FTIR can be envisioned three ways. A first approach consists of a visual presorting; in this case, the attenuate total reflection (ATR) crystal is focused on every single particle.<sup>6,11,21,34</sup> The visual presorting and focusing is very time consuming. In a second approach, the automated image analysis of the filter is proposed. This consists of the detection and localization of the particles prior to characterization.<sup>25</sup> The third option is a spectroscopic mapping of the whole surface of the filter.<sup>14,15</sup> In this later case, the bands selected to detect the plastic have to be chosen among polymer specific regions that are insensitive to variations in the particle shape or state of oxidation.<sup>10</sup> To control the amount of data generated, the region for the IR scanning is also restricted to some specific polymer bands, and the number of scans per measurement, thus the resolution of the measurements, is lower. All these options affect the signal/noise ratio, and these adjustments are detrimental to the reliability of the measure. Primpke et al. developed software to analyze and interpret the very voluminous data generated by the mapping.<sup>25</sup>

Here, we opted for the  $\mu$  FTIR characterization with a visual presorting and a systematic crystal focus on every single particle. The spectra were much better compared to the automated method. We decided to analyze the whole surface of the filter because it presented very important heterogeneity. In contrast, this option utilized an operator for a long time and thus was accompanied by an operator bias that was difficult to estimate. Lines with diameters a few hundreds of micron and a few millimeter big were present in the LMP samples. Line probably comes from the degradation of fishing lines or gears. Textile fibers present much smaller diameters, tens of microns, they belong to the SMP category. But because fibers do not deposit flat on the surface of the filter (a part of the fiber is out of focus of the IRbeam) they are hardly detectable and their infrared spectra does not allow a correct correspondence with the library.<sup>35</sup> We presume that this method underestimated SMP abundance, and we acknowledge that this method needs further methodological improvement to make the analysis more reliable.

LMP (960 particles isolated in total) were made of 90% PE and 10% PP; this is in agreement with reported data from the open ocean.<sup>26</sup> SMP (1 100 particles isolated in total) were made of a greater diversity of polymers, as has already reported.<sup>21</sup> SMP were made of PE (70%), PP (17%), PVC (7%), PS (1%), PET (1%) and to a lesser extent polyurethane, poly aryl ether sulfone and phenoxy resins ([Figure 1](#)). However, polyolefins were still predominant. SMP repartition among polymer types presented variation along the sampling locations ([SI Table S1](#)). For example, at station 12, 98% of the SMP were made of PE, while at station 20, only 41% were made of PE and 51% of PP. A contribution of 13% of PVC particles was identified at station 24. Finally, for all sampling points, PS and PET proportions never exceeded 5%.

**Modeling Approach and Validation.** LMP concentrations at the sea surface are usually corrected using the modeling approach introduced by Kukulka et al.<sup>19</sup> This model is based on the number of microplastics collected at the surface ( $N_{\text{low}}$ ), the rise velocity ( $W_b$ ) and the surface forcing (wind and waves), which is based on the friction velocity of water

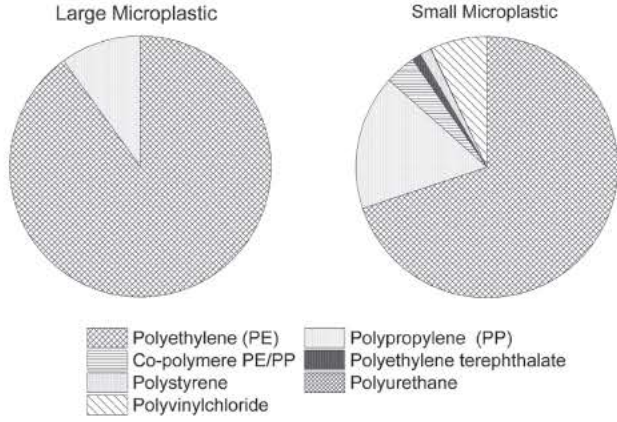


**Figure 1.** Relative proportion of the polymer found among the large microplastic (1–5 mm) and small microplastic (25–1000  $\mu\text{m}$ ) collected during the sea campaign Expedition 7<sup>th</sup> Continent.

( $u_{*w}$ ). This last parameter is calculated from the mean wind velocity at  $z = 10$  m ( $U_{10}$ ) assuming a log velocity profile<sup>36</sup> and using parametric expressions.<sup>37,38</sup> Without any assumption about the turbulent forcing (by comparing  $u_{*w}$  to  $W_b$ ), we note  $f$  the correction factor that compares, at a given location, the estimate of the corrected concentration in count ( $N$ ) to  $N_{\text{tow}}$ :

$$f = \frac{N}{N_{\text{tow}}} = \frac{1}{1 - \exp\left(-\frac{dW_b}{A_0}\right)} \quad (1)$$

where  $d$  is the net's immersion depth,  $A_0 = 1.5u_{*w}\kappa H_s$  is an empirical parametrization for the near surface mixing<sup>37</sup> with  $\kappa = 0.4$  being the Karman constant and  $H_s = 0.96\sigma^{3/2}u_{*a}^2$  being the significant wave height. The  $H_s$  model was proposed by Thorpe et al.,<sup>37</sup> where  $\sigma$  is the wave age and  $u_{*a}$  the friction velocity of air derived from  $U_{10}$ .<sup>38</sup> The assumption of a fully developed sea is done<sup>19,39</sup> by taking a constant wave age,  $\sigma = 35$ . As a remark, the influence of the choice of wave model on  $f$  is weak compared to the influence of the plastic geometry (SI Section S3).

The steady rise velocity for a plastic particle in a fluid at rest can be modeled by balancing the buoyancy force with the drag exerted on the particle,

$$\frac{1}{2}\rho C_D(Re)SW_b^2 = (\rho_p - \rho)Vg \quad (2)$$

where  $\rho_p$  and  $\rho$  are the densities of the particle and the fluid, respectively,  $g$  is the gravitational constant,  $C_D$  is the drag coefficient,  $Re$  is the Reynolds number defined by a characteristic length scale times a characteristic velocity (here  $W_b$ ) of the particle divided by  $\nu$ , which is the fluid kinematic viscosity,  $S$  is the area of the apparent section of the particle, and  $V$  is its volume. Recently, Enders et al. envisioned this approach for a spherical geometry.<sup>21</sup> eq 2 is implicit for  $W_b$ , and the solution strongly depends on the density,  $\rho_p$ , and on the geometry of the particle through  $S$ ,  $V$ , and more specifically,  $C_D$ . Although any shape can be studied with eq 2 by modifying the version of the sphere model,<sup>40</sup> we chose to express an upper and a lower bound for  $W_b$  by determining geometries that properly describe plastic particle shapes. The modeling approach to characterize dynamics of slender lines is much more complicated. Depending on the flexibility of the fiber, its orientation and shape could be modified in time when buckling occurs, changing its rise velocity, while it is not the case for a rigid body.<sup>41</sup> The steady rise velocity is also difficult to estimate from the calculation because intrinsic properties of each line are also needed (elastic modulus more specifically) and no proper model such as for the drag coefficient is known. At this time we prefer to exclude lines from our calculations. As noted earlier, fibers are also very difficult to detect by  $\mu$  FTIR.<sup>35</sup>

Based on the full characterization ( $L, l, h$ ) of 451 microplastics (SI Section S2), we propose to encompass any particle's shape by two model geometries. We selected our first geometry as a sphere based on the equivalent radius  $R_{\text{eq}} = \sqrt{LI/\pi}$  and our second geometry as an ellipsoid based on the equivalent half axis  $L_{\text{eq}} = \sqrt{LI/4}$  and the aspect ratio  $\chi = L/h = 10$ . The statistical distribution for the values of  $\chi$  for the 415 microplastics showed that most of them (95%) are consistent with the sphere and an ellipsoid models with aspect ratios between 1 (sphere) and 10 (SI Figure S1). We emphasize here that using  $L_{\text{eq}}$  instead of  $L$ , the longest dimension of the plastic particle, to represent the distribution of concentration in count is a better parameter allowing for a continuous size distribution (SI Section S5). In the following discussion, we will use  $L_{\text{eq}}$  preferentially.

The density of plastic particles is another important parameter for particle dynamics. Most of the plastic particles collected in the open ocean (92%) present a density between 0.9 and 1.0 g  $\text{cm}^{-3}$ .<sup>42</sup> For a given density, the ellipsoid rises

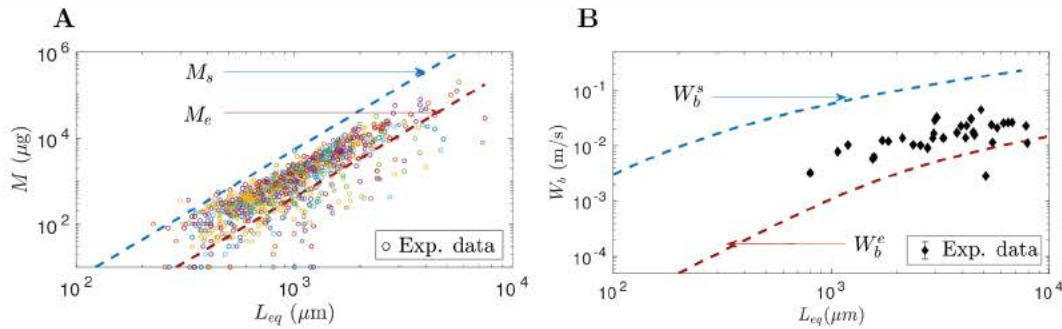


**Figure 2.** (A) Mass of 900 LMP (symbols) as a function of their characteristic length scale,  $L_{\text{eq}} = \sqrt{LI/4}$ ; the corresponding estimates for the sphere ( $M_s$ ) and the ellipsoid ( $M_e$ ) models are shown with blue and red dashed curves, respectively. Each symbol's color corresponds to a net tow. (B) Rise velocity measurements of 35 microplastics (symbols) compared to estimates for the sphere ( $W_b^s$ ) and the ellipsoid ( $W_b^e$ ) models shown in blue and red, respectively.

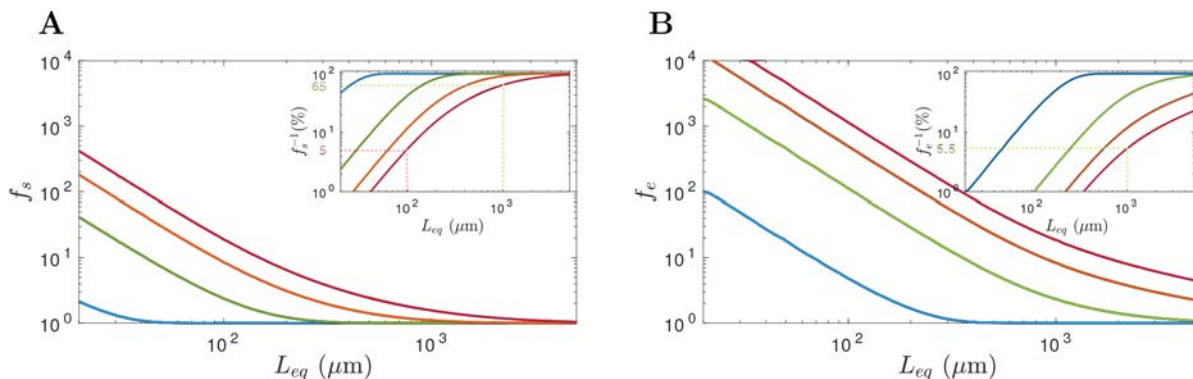


**Figure 3.** Correction factors estimated for (A) the sphere model ( $f_s$ ) and (B) the ellipsoid model ( $f_e$ ) calculated for a net immersion depth of 20 cm. Each color corresponds to a Beaufort (blue: Beaufort 1–2, green: Beaufort 3, orange: Beaufort 4, and magenta: Beaufort 5). Inset plots correspond to the theoretical fraction of surface captured plastic particles ( $f^{-1}$ ) in percent at [0–20] cm.

slower than the sphere with  $R_{eq} = L_{eq}$ . Thus, to encompass the dynamics of microplastics, we attributed to the ellipsoid density the upper limit ( $1.005 \text{ g cm}^{-3}$ ), and to the sphere density, the lower limit ( $0.900 \text{ g cm}^{-3}$ ). We note that  $M_e$  and  $M_s$  are the corresponding masses for the ellipsoid and sphere geometries. The drag coefficient models and corresponding resolution of eq 2 for these objects are presented in SI Section S4.

As a first validation of the model, we compared the mass of the LMP to the calculated mass of the sphere and the ellipsoid. The majority of LMP mass (85%) fell within the delimited boundaries (Figure 2A). Since we could not weigh the SMP, we assumed that the two geometries described the SMP well, and we used the average mass,  $M_m = (M_e + M_s)/2$ , to provide a mass estimate for the direct observations. As a second validation, we compared the calculated rise velocity of the ellipsoid,  $W_b^e$ , and the sphere,  $W_b^s$ , to the rise velocity of 35 arbitrarily selected LMP. Their rise velocities were measured in laboratory conditions with a system that avoided the generation of any turbulence during the introduction of the particle into the water column (Figure 2B). The majority (97%) had a rise velocity between  $W_b^e$  and  $W_b^s$ . Only one object was out of bounds, it turned out to have an aspect ratio larger than 10, which is consistent with a smaller rising velocity. We calculated  $W_b$  for a wide range of microplastic sizes. However, our calculations of  $W_b$  were in the same range as those measured previously ( $>0.5 \text{ mm}$ ).<sup>19,22</sup> It was not possible to measure the rise velocity of SMP because they were too small to be handled. Nonetheless, eq 2 is also valid in the micrometric range. For SMP, the calculated values for  $W_b$  are between  $3 \times 10^{-3}$  and  $10^{-4} \text{ m s}^{-1}$ . These are 1–2 orders of magnitude below the mean value for LMP. This finding well illustrates the importance of integrating the variations of  $W_b$  into the turbulence model.

Using eq 1, we define  $f_e$  and  $f_s$  as the correction factors associated with the ellipsoid and the sphere, respectively (Figure 3A and B). As smaller particles present lower buoyancy at a given sea state, their correction factors are higher. For example, at Beaufort 1, 100% of the plastic particles with  $L_{eq} > 1 \text{ mm}$  are within the first 20 cm ( $f_e = f_s = 1$ ), while when  $L_{eq} = 100 \mu\text{m}$ , only between 20 and 100% are within the first 20 cm ( $f_e = 5$  and  $f_s = 1$ ). The corrections proposed by previous studies for LMP fell within the interval proposed here (data not shown).<sup>19,22</sup> It must be noted that this difference between small and large microplastic distributions in the water column increases with the Beaufort. For instance, at Beaufort 5,

between 5.5 and 65% of plastic particles with  $L_{eq} = 1 \text{ mm}$  are located within the surface layer, but only between 1 and 5% of plastic particles with  $L_{eq} = 100 \mu\text{m}$  are (inset plots Figures 3A and B). In these conditions, the corrections could lead to major error estimates, which is why we excluded stations at Beaufort 5 from the following discussion (Tables 1 and 2).

**Table 1. Concentration in Count ( $\times 10^5 \text{ Particles km}^{-2}$ ) for LMP (1–5 mm) and SMP (25–1000  $\mu\text{m}$ ) at Eight Sampling Stations (detailed information available in SI Table S1), Lines and Fibers Excluded<sup>a</sup>**

#	Beaufort	1–5 mm			25–1000 $\mu\text{m}$		
		$N_{\text{low}}$	$N_{\text{corr}}^s$	$N_{\text{corr}}^e$	$N_{\text{low}}$	$N_{\text{corr}}^s$	$N_{\text{corr}}^e$
6	5	0.14			24		
8	5	0.18			12		
11	3	0.13	0.13	0.27	7.9	870	41 000
12	5	0.14			11		
17	3	0.38	0.40	1.13	6.3	730	34 000
20	3	0.98	0.98	3.20	5.0	600	24 000
24	2	1.74	1.74	1.88	60	750	36 000
27	3	0.34	0.34	0.66	3.8	110	45 000
mean		0.50	0.72	1.43	16.3	610	36 000

<sup>a</sup> $N_{\text{low}}$  is the uncorrected concentration in count, and  $N_{\text{corr}}^i$  is the corrected concentration in count, where superscript  $i$  refers to the model used for correction ( $s$  for the sphere model and  $e$  for the ellipsoid model).

Our modeling approach allows us to relate count and weight concentrations evaluations. For each sample, an estimated mass can be provided, and for the sake of simplicity, we chose the average mass of the two geometries,  $M_m$ . For a given  $L_{eq}$ , the corrected concentrations in weight are obtained by multiplying  $M_m$  with the correction factors  $f_e$  and  $f_s$  (Table 2).

**Measured Count and Weight Concentrations.** Averaged LMP and SMP concentrations in count without correction were  $50\,000 \text{ particles km}^{-2}$  and  $1\,630\,000 \text{ particles km}^{-2}$ , respectively. LMP concentrations were between  $13\,000$  and  $174\,000 \text{ particles km}^{-2}$ , while SMP concentrations were between  $630\,000$  and  $6\,000\,000 \text{ particles km}^{-2}$  (Table 1). The highest concentrations for both LMP and SMP were measured for station 24 at low wind speed (Beaufort 2). LMP concentrations in count were typical of the ones encountered in subtropical gyres.<sup>43–46</sup> Concerning SMP concentrations, there are no data for comparison. The global trend over these 8 sampling stations was that there were between 5 and 171 times

**Table 2. Concentration in Weight ( $\text{g km}^{-2}$ ) for LMP (1–5 mm) and SMP (25–1000  $\mu\text{m}$ ) Associated with Table 1<sup>a,b</sup>**

#	Beaufort	1 5 mm			25 1000 $\mu\text{m}$		
		$M_{\text{tow}}$	$M_{\text{corr}}^s$	$M_{\text{corr}}^e$	$M_{\text{tow}}$	$M_{\text{corr}}^s$	$M_{\text{corr}}^e$
6	5	35.3			5.9		
8	5	57.4			3.2		
11	3	46.6	50	400	0.8	64	2900
12	5	16.8			0.8		
17	3	214	220	1000	0.6	32	2100
20	3	194	230	1400	0.4	5.2	110
24	2	180	180	340	44	410	14000
27	3	63.9	64	600	5.0	58	2000
Mean		100	150	750	7.6	110	4200

<sup>a</sup>The SMP uncorrected concentrations in weight are extrapolated from the models. <sup>b</sup> $M_{\text{tow}}$  is the uncorrected concentration in weight, and  $M_{\text{corr}}^i$  is the corrected concentration in weight, where super script  $i$  refers to the model used for correction ( $s$  for the sphere model and  $e$  for the ellipsoid model).

more SMP than LMP. We could not identify a specific correlation in their respective distributions. The heterogeneities observed at equivalent sea states could eventually be rationalized by mesoscale ocean dynamics.<sup>27</sup>

Uncorrected concentrations in weight are given in Table 2. On average, they are  $100 \text{ g km}^{-2}$  for LMP and  $7.6 \text{ g km}^{-2}$  for SMP. For LMP, the values fell within reported data,<sup>45</sup> and for SMP, there are no data for comparison. As observed with concentrations in count, the lowest concentrations in weight were measured at the highest wind speed conditions (from stations 6 through 12), and the highest ones were measured under the best sea state conditions (from stations 17 through 27). As a global trend, uncorrected SMP concentrations in weight were 10 to 100 times lower than those of LMP.

**Corrected Count and Weight Concentrations.** Corrected LMP concentrations in count were between 13 000 and 188 000 particles  $\text{km}^{-2}$ , whereas for SMP, they were between 60 million and 4.5 billion particles  $\text{km}^{-2}$  (Table 1). For LMP, correction factors were between 1 and 3.3 and were much higher for SMP, between 12.5 and 11 800. Without correction, SMP were between 5 and 171 times more abundant than LMP. After correction, SMP were between 30 000 and 70 000 times more abundant than LMP. There does not seem to be any correlation between LMP and SMP concentrations in count after correction. Averaged corrected LMP concentrations in weight were between 150 and  $750 \text{ g km}^{-2}$  for the lower and upper corrections; for SMP, they were between 110 and  $4200 \text{ g km}^{-2}$ . Station 24 is notable; at this location, the concentrations are remarkably high, and the corrected SMP concentrations in weight were estimated to be between 0.4 and  $14 \text{ kg km}^{-2}$ . As a remark, for both SMP and LMP, all concentrations in weight were about a few hundred grams up to a few kilos per square kilometer.

**Implications.** The present study demonstrates that SMP are very abundant and that their concentration in weight is of the same order of magnitude as that of LMP. The present model supplies correction with lower and upper bounds. It does not include the biofilm that could modify the density and the dimension of the particle, a future implementation of this model could be the introduction of the biofilm, but it needs a complete parametrization of the biofilm before. A global estimation of what small microplastic mass would represent needs further in situ data. The actual detection and

quantification method by  $\mu$  FTIR needs automatization to reduce the cost and time of analysis and to produce more field data. The quantification of nanoplastic has not been developed yet and the contribution of nanoplastic to plastic mass balance is for the moment only speculative.

The intervals for SMP, supplied by the current model, are wide and upper bounds for LMP are much larger than previous models. This finding illustrates the uncertainty in the sampling strategy at the sea surface. Due to reduced buoyancy, SMP are more susceptible to vertical transport. Their abundance in the subsurface was described at 3 or 10 m depth.<sup>21,47</sup> A better description of SMP distribution in the water column requires depth profile measurements even if there are some logistical aspect that should be fixed due to the important volume of water that should be filtered. Furthermore, the hypothesis of a balance between the buoyant upward flux and the turbulent downward flux could no longer be extrapolated for the smallest plastic particles. Indeed, down to a given size (still to be defined), they become passive tracers for the turbulence,<sup>5</sup> and their vertical distribution in the water could be set by a different modeling approach.<sup>48,49</sup>

## ■ ASSOCIATED CONTENT

### ● Supporting Information

The Supporting Information is available free of charge on the ACS Publications website at DOI: 10.1021/acs.est.8b05458.

Net tow information (Section S1), geometrical description of collected plastic samples (Section S2), influence of the significant wave height model (Section S3), drag model (Section S4) and size distribution (Section S5) (PDF)

## ■ AUTHOR INFORMATION

### Corresponding Author

\*E mail: [ter\\_halle@chimie.ups.tlse.fr](mailto:ter_halle@chimie.ups.tlse.fr).

### ORCID

Alexandra ter Halle: 0000 0001 7065 2272

### Notes

The authors declare no competing financial interest. The modeling approach presented in the manuscript is implemented in an open source software “plasticcount” freely available at <https://sourceforge.net/projects/plasticcount/>.

## ■ ACKNOWLEDGMENTS

The project is supported by the Total Corporate Foundation and the Centre National d’Etudes Spatiales (CNES). We thank the association Expedition 7<sup>th</sup> Continent for the sea sampling campaign, the staff and the crew.

## ■ REFERENCES

- (1) Jambeck, J. R.; Geyer, R.; Wilcox, C.; Siegler, T. R.; Perryman, M.; Andrady, A.; Narayan, R.; Law, K. L. Marine pollution. Plastic waste inputs from land into the ocean. *Science* 2015, 347, 768–771.
- (2) Geyer, R.; Jambeck, J. R.; Law, K. L. Production, use, and fate of all plastics ever made. *Science Advances* 2017, 3, No. e1700782.
- (3) Gigault, J.; Pedrono, B.; Maxit, B.; Ter Halle, A. Marine plastic litter: the unanalyzed nano fraction. *Environ. Sci.: Nano* 2016, 3, 346–350.
- (4) Filella, M. Questions of size and numbers in environmental research on microplastics: methodological and conceptual aspects. *Environ. Chem.* 2015, 12, 527–538.

- (5) Gigault, J.; ter Halle, A.; Baudrimont, M.; Pascal, P. Y.; Gauffre, F.; Phi, T. L.; El Hadri, H.; Grassl, B.; Reynaud, S. What is a nanoplastic? *Environ. Pollut.* **2018**, *235*, 1030–1034.
- (6) Song, Y. K.; Hong, S. H.; Jang, M.; Han, G. M.; Rani, M.; Lee, J.; Shim, W. J. A comparison of microscopic and spectroscopic identification methods for analysis of microplastics in environmental samples. *Mar. Pollut. Bull.* **2015**, *93*, 202–209.
- (7) Bergmann, M.; Wirzberger, V.; Krumpfen, T.; Lorenz, C.; Primpke, S.; Tekman, M. B.; Gerdt, G. High Quantities of Microplastic in Arctic Deep Sea Sediments from the HAUSGARTEN Observatory. *Environ. Sci. Technol.* **2017**, *51*, 11000–11010 PMID: 28816440 .
- (8) Cauwenberghe, L. V.; Devriese, L.; Galgani, F.; Robbens, J.; Janssen, C. R. Microplastics in sediments: A review of techniques, occurrence and effects. *Mar. Environ. Res.* **2015**, *111*, 5–17.
- (9) Hanvey, J. S.; Lewis, P. J.; Lavers, J. L.; Crosbie, N. D.; Pozo, K.; Clarke, B. O. A review of analytical techniques for quantifying microplastics in sediments. *Anal. Methods* **2017**, *9*, 1369–1383.
- (10) Harrison, J. P.; Ojeda, J. J.; Romero Gonzalez, M. E. The applicability of reflectance micro Fourier transform infrared spectroscopy for the detection of synthetic microplastics in marine sediments. *Sci. Total Environ.* **2012**, *416*, 455–463.
- (11) Imhof, H. K.; Schmid, J.; Niessner, R.; Ivleva, N. P.; Laforsch, C. A novel, highly efficient method for the separation and quantification of plastic particles in sediments of aquatic environments. *Limnol. Oceanogr.: Methods* **2012**, *10*, 524–537.
- (12) Lenz, R.; Enders, K.; Stedmon, C. A.; Mackenzie, D. M. A.; Nielsen, T. G. A critical assessment of visual identification of marine microplastic using Raman spectroscopy for analysis improvement. *Mar. Pollut. Bull.* **2015**, *100*, 82–91.
- (13) Tagg, A. S.; Sapp, M.; Harrison, J. P.; Ojeda, J. J. Identification and Quantification of Microplastics in Wastewater Using Focal Plane Array Based Reflectance Micro FT IR Imaging. *Anal. Chem.* **2015**, *87*, 6032–6040.
- (14) Loeder, M. G. J.; Kuczera, M.; Mintenig, S.; Lorenz, C.; Gerdt, G. Focal plane array detector based micro Fourier transform infrared imaging for the analysis of microplastics in environmental samples. *Environ. Chem.* **2015**, *12*, 563–581.
- (15) Vianello, A.; Boldrin, A.; Guerriero, P.; Moschino, V.; Rella, R.; Sturaro, A.; Da Ros, L. Microplastic particles in sediments of Lagoon of Venice, Italy: First observations on occurrence, spatial patterns and identification. *Estuarine, Coastal Shelf Sci.* **2013**, *130*, 54–61.
- (16) Mintenig, S. M.; Int Veen, I.; Loeder, M. G. J.; Primpke, S.; Gerdt, G. Identification of microplastic in effluents of waste water treatment plants using focal plane array based micro Fourier transform infrared imaging. *Water Res.* **2017**, *108*, 365–372.
- (17) van Wezel, A.; Caris, I.; Kools, S. A. E. Release of primary microplastics from consumer products to wastewater in the Netherlands. *Environ. Toxicol. Chem.* **2016**, *35*, 1627–1631.
- (18) Kukulka, T.; Law, K. L.; Proskurowski, G. Evidence for the Influence of Surface Heat Fluxes on Turbulent Mixing of Microplastic Marine Debris. *J. Geophys. Res. Oceans* **2016**, *46*, 809–815.
- (19) Kukulka, T.; Proskurowski, G.; Meyer, D. W.; Law, K. L.; et al. The effect of wind mixing on the vertical distribution of buoyant plastic debris. *Geophys. Res. Lett.* **2012**, *39*, 1–6.
- (20) Kukulka, T.; Brunner, K. Passive buoyant tracers in the ocean surface boundary layer: 1. Influence of equilibrium wind waves on vertical distributions. *J. Geophys. Res. Oceans* **2015**, *120*, 3837–3858.
- (21) Enders, K.; Lenz, R.; Stedmon, C. A.; Nielsen, T. G. Abundance, size and polymer composition of marine microplastics  $\geq 10 \mu\text{m}$  in the Atlantic Ocean and their modelled vertical distribution. *Mar. Pollut. Bull.* **2015**, *100*, 70–81.
- (22) Reisser, J.; Slat, B.; Noble, K.; Du Plessis, K.; Epp, M.; Proietti, M.; De Sonneville, J.; Becker, T.; Pattiaratchi, C. The vertical distribution of buoyant plastics at sea: An observational study in the North Atlantic Gyre. *Biogeosciences* **2015**, *12*, 1249–1256.
- (23) Law, K. L. Plastics in the Marine Environment. *Annu. Rev. Mar. Sci.* **2017**, *9*, 205–229 PMID: 27620829 .
- (24) Ter Halle, A.; Jeanneau, L.; Martignac, M.; Jarde, E.; Pedrono, B.; Brach, L.; Gigault, J. Nanoplastic in the North Atlantic Subtropical Gyre. *Environ. Sci. Technol.* **2017**, *51*, 13689–13697.
- (25) Primpke, S.; Lorenz, C.; Rascher Friesenhausen, R.; Gerdt, G. An automated approach for microplastics analysis using focal plane array (FPA) FTIR microscopy and image analysis. *Anal. Methods* **2017**, *9*, 1499–1511.
- (26) Ter Halle, A.; Ladirat, L.; Gendre, X.; Goudouneche, D.; Pusineri, C.; Routaboul, C.; Tenailleau, C.; Duployer, B.; Perez, E. Understanding the Fragmentation Pattern of Marine Plastic Debris. *Environ. Sci. Technol.* **2016**, *50*, 5668–5675.
- (27) Brach, L.; Deixonne, P.; Bernard, M. F.; Durand, E.; Desjean, M. C.; Perez, E.; van Sebille, E.; ter Halle, A. Anticyclonic eddies increase accumulation of microplastic in the North Atlantic subtropical gyre. *Mar. Pollut. Bull.* **2018**, *126*, 191–196.
- (28) Claessens, M.; De Meester, S.; Van Landuyt, L.; De Clerck, K.; Janssen, C. R. Occurrence and distribution of microplastics in marine sediments along the Belgian coast. *Mar. Pollut. Bull.* **2011**, *62*, 2199–2204.
- (29) Nuelle, M. T.; Dekiff, J. H.; Remy, D.; Fries, E. A new analytical approach for monitoring microplastics in marine sediments. *Environ. Pollut.* **2014**, *184*, 161–169.
- (30) Imhof, H. K.; Laforsch, C.; Wiesheu, A. C.; Schmid, J.; Anger, P. M.; Niessner, R.; Ivleva, N. P. Pigments and plastic in limnetic ecosystems: A qualitative and quantitative study on microparticles of different size classes. *Water Res.* **2016**, *98*, 64–74.
- (31) Foekema, E. M.; De Groot, C. J.; Mergia, M. T.; van Franeker, J. A.; Murk, A. J.; Koelmans, A. A. Plastic in North Sea Fish. *Environ. Sci. Technol.* **2013**, *47*, 8818–8824.
- (32) Cole, M.; Webb, H.; Lindeque, P. K.; Fileman, E. S.; Halsband, C.; Galloway, T. S. Isolation of microplastics in biota rich seawater samples and marine organisms. *Sci. Rep.* **2015**, *4*, 4528.
- (33) Kaeppler, A.; Fischer, D.; Oberbeckmann, S.; Schernewski, G.; Labrenz, M.; Eichhorn, K. J.; Voit, B. Analysis of environmental microplastics by vibrational microspectroscopy: FTIR, Raman or both? *Anal. Bioanal. Chem.* **2016**, *408*, 8377–8391.
- (34) Cauwenberghe, L. V.; Vanreusel, A.; Mees, J.; Janssen, C. R. Microplastic pollution in deep sea sediments. *Environ. Pollut.* **2013**, *182*, 495–499.
- (35) Peeken, I.; Primpke, S.; Beyer, B.; Guetermann, J.; Katlein, C.; Krumpfen, T.; Bergmann, M.; Hehemann, L.; Gerdt, G. Arctic sea ice is an important temporal sink and means of transport for microplastic. *Nat. Commun.* **2018**, *9*, 1505.
- (36) Smith, S. D. Coefficients for sea surface wind stress, heat flux, and wind profiles as a function of wind speed and temperature. *J. Geophys. Res.* **1988**, *93*, 15467–15472.
- (37) Thorpe, S.; Osborn, T. R.; Farmer, D. M.; Vagle, S. Bubble Clouds and Langmuir Circulation: Observations and Models. *J. Phys. Oceanogr.* **2003**, *33*, 2013–2031.
- (38) Smith, S. D. Wind Stress and Heat Flux over the Ocean in Gale Force Winds. *J. Phys. Oceanogr.* **1980**, *10*, 709–726.
- (39) Fan, Y.; Hwang, P. Kinetic energy flux budget across air sea interface. *Ocean Model.* **2017**, *120*, 27–40.
- (40) Clip, R.; Grace, J. R.; Weber, M. E. *Bubbles, Drops, and Particles*; Academic Press: United Kingdom, 1978.
- (41) Li, L.; Manikantan, H.; Spagnolie, S. E. The sedimentation of flexible filaments. *J. Fluid Mech.* **2013**, *735*, 705–736.
- (42) Morét Ferguson, S.; Law, K. L.; Proskurowski, G.; Murphy, E. K.; Peacock, E. E.; Reddy, C. M. The size, mass, and composition of plastic debris in the western North Atlantic Ocean. *Mar. Pollut. Bull.* **2010**, *60*, 1873–1878.
- (43) Law, K. L.; Morét Ferguson, S. E.; Maximenko, N. A.; Proskurowski, G.; Peacock, E. E.; Hafner, J.; Reddy, C. M. Plastic Accumulation in the North Atlantic Subtropical Gyre. *Science* **2010**, *329*, 1185–1188.
- (44) Law, K. L.; Morét Ferguson, S. E.; Goodwin, D. S.; Zettler, E. R.; Deforce, E.; Kukulka, T.; Proskurowski, G. Distribution of surface

plastic debris in the eastern pacific ocean from an 11 year data set. *Environ. Sci. Technol.* **2014**, *48*, 4732–4738.

(45) Cozar, A.; Echevarria, F.; Gonzalez Gordillo, J. I.; Irigoien, X.; Ubeda, B.; Hernandez Leon, S.; Palma, A. T.; Navarro, S.; Garcia de Lomas, J.; Ruiz, A.; Fernandez de Puellas, M. L.; Duarte, C. M. Plastic debris in the open ocean. *Proc. Natl. Acad. Sci. U. S. A.* **2014**, *111*, 10239–10244.

(46) Eriksen, M.; Lebreton, L. C.; Carson, H. S.; Thiel, M.; Moore, C. J.; Borerro, J. C.; Galgani, F.; Ryan, P. G.; Reisser, J. Plastic Pollution in the World's Oceans: More than 5 Trillion Plastic Pieces Weighing over 250,000 Tons Afloat at Sea. *PLoS One* **2014**, *9*, 1–15.

(47) Kanhai, L. D. K.; Officer, R.; Lyashevskaya, O.; Thompson, R. C.; O'Connor, I. Microplastic abundance, distribution and composition along a latitudinal gradient in the Atlantic Ocean. *Mar. Pollut. Bull.* **2017**, *115*, 307–314.

(48) Michallet, H.; Mory, M. Modelling of sediment suspensions in oscillating grid turbulence. *Fluid Dyn. Res.* **2004**, *35*, 87–106.

(49) Huppert, H. E.; Turner, J. S.; Hallworth, M. A. Sedimentation and entrainment in dense layers of suspended particles by an oscillating grid. *J. Fluid Mech.* **1995**, *289*, 263–293.